Title

Linoleic acid-derived 13-hydroxyoctadecadienoic acid is absorbed and incorporated into rat tissues

Journal

Biochimica et Biophysica Acta (BBA) - Molecular and Cell Biology of Lipids, 1866(3)

ISSN

1388-1981

Authors

Zhang, Zhichao
Emami, Shiva
Hennebelle, Marie
et al.

Publication Date

2021-03-01

DOI

10.1016/j.bbalip.2020.158870

Peer reviewed

BBA - Molecular and Cell Biology of Lipids 1866 (2021) 158870

Contents lists available at ScienceDirect

BBA - Molecular and Cell Biology of Lipids

journal homepage: www.elsevier.com/locate/bbalip

Linoleic acid-derived 13-hydroxyoctadecadienoic acid is absorbed and incorporated into rat tissues

Zhichao Zhang [a], Shiva Emami [a], Marie Hennebelle [a,1], Rhianna K. Morgan [b], Larry A. Lerno [c], Carolyn M. Slupsky [a,d], Pamela J. Lein [b], Ameer Y. Taha [a,*]

[a] Department of Food Science and Technology, College of Agriculture and Environmental Sciences, University of California, Davis, CA, USA
[b] Department of Molecular Biosciences, School of Veterinary Medicine, University of California, Davis, CA, USA
[c] Food Safety and Measurement Facility, University of California, Davis, CA, USA
[d] Department of Nutrition, College of Agriculture and Environmental Sciences, University of California, Davis, CA, USA

ARTICLE INFO

Keywords:
Oxidized linoleic acid metabolites (OXLAMs)
Brain
Heart
Liver
Adipose tissue
Kinetics

ABSTRACT

Linoleic acid (LNA)-derived 13-hydroxyoctadecadienoic acid (13-HODE) is a bioactive lipid mediator that regulates multiple signaling processes in vivo. 13-HODE is also produced when LNA is oxidized during food processing. However, the absorption and incorporation kinetics of dietary 13-HODE into tissues is not known. The present study measured unesterified d4-13-HODE plasma bioavailability and incorporation into rat liver, adipose, heart and brain following gavage or intravenous (IV) injection (n = 3 per group). Mass spectrometry analysis revealed that d4-13-HODE was absorbed within 20 min of gavage, and continued to incorporate into plasma esterified lipid fractions throughout the 90 min monitoring period (incorporation half-life of 71 min). Following IV injection, unesterified d4-13-HODE was rapidly eliminated from plasma with a half-life of 1 min. Analysis of tracer incorporation kinetics into rat tissues following IV injection or gavage revealed that the esterified tracer preferentially incorporated into liver, adipose and heart compared to unesterified d4-13-HODE. No tracer was detected in the brain. This study demonstrates that dietary 13-HODE is absorbed, and incorporated into peripheral tissues from esterified plasma lipid pools. Understanding the chronic effects of dietary 13-HODE exposure on peripheral tissue physiology and metabolism merits future investigation.

1. Introduction

Omega-6 linoleic acid (LNA, 18:2 n-6) is a precursor to bioactive oxidized linoleic acid metabolites (OXLAMs) generated in vivo via autooxidation, or enzymatically through lipoxygenase (LOX), cyclooxygenase (COX), cytochrome P450 (CYP) and soluble epoxide hydrolase (sEH) [1–6]. OXLAMs have multiple biological roles including the regulation of pain threshold [7], inflammation [8,9], apoptosis [10], cardiac activity [11], adipocyte fatty acid uptake and thermogenesis [12], neurotransmission [13] and neuronal morphogenesis [14].

Previously, we reported that dietary LNA regulates circulating OXLAM concentrations in humans [15], as well as plasma and tissue levels in rodents [16]. Increasing dietary LNA corresponded to incremental increases in plasma and tissue OXLAM concentrations, suggesting that dietary LNA plays a key role in regulating in vivo OXLAM levels [17].

OXLAMs are also present in the diet, raising the possibility that they might contribute directly to in vivo OXLAM concentrations. Studies reported the presence of OXLAMs in non-heated soybean, canola, corn, olive, flaxseed and algae oils [18], and in bovine and human breast milk [19–21]. Thermal treatment of oils used in food processing has been shown to markedly increase OXLAM concentrations [22].

Abbreviations: COX, cyclooxygenase; CYP450, cytochrome *p*450; ARA, arachidonic acid; PGE, prostaglandin; EPA, eicosapentaenoic acid; UE, unesterified; ES, esterified; LNA, linoleic acid; LOX, lipoxygenase; OXLAMs, oxidized linoleic acid metabolites; PG, Prostaglandin; sEH, soluble epoxide hydrolase; SPE, solid phase extraction; IV, intravenous; 13-HODE, 13-hydroxyloctadecadienoic acid; UPLC-MS/MS, ultra-high performance liquid chromatography coupled to tandem mass-spectrometry.

* Corresponding author at: Department of Food Science and Technology, College of Agriculture and Environmental Sciences, University of California Davis, One Shields Avenue, RMI North (3162), Davis, CA 95616, USA.
E-mail address: ataha@ucdavis.edu (A.Y. Taha).
[1] Current address: Laboratory of Food Chemistry, Wageningen University and Research, Wageningen, Netherlands.

https://doi.org/10.1016/j.bbalip.2020.158870
Received 7 June 2020; Received in revised form 22 October 2020; Accepted 14 December 2020
Available online 17 December 2020

The contribution of dietary OXLAMs to circulating and tissue levels is not clearly known due to conflicting studies on their bioavailability [16]. Bergan and Draper detected radioactivity in liver and mesenteric adipose of rats 24 h after gavage with ^{14}C-labeled 13- hydroperoxyoctadecadienoic acid; however, the chemical identity of the radioactive compounds that accumulated in liver and adipose is not known [23]. Kanazawa et al. showed that ^{14}C-labeled 13- hydroperoxyoctadecadienoic acid was converted in the stomach into LNA hydroxy and epoxyketones, which further degraded to aldehydes before reaching the small intestines [24]. Another study showed that more LNA hydroxy metabolites appeared in lymphatic tissue compared to LNA hydroperoxides following intragastric administration [25]. The overall evidence suggests that OXLAMs may be absorbed, but it is not known if they remain intact once in the body.

Recently, we reported that plasma and brain OXLAM concentrations were not altered in mice fed a high OXLAM diet derived from thermally oxidized corn oil, for 8 weeks [9,16]. The lack of change in plasma and tissue OXLAM concentrations following dietary OXLAM feeding could be due to 1) limited absorption, 2) conversion into other ketone or hydroxylated compounds as previously suggested [24], and/or 3) rapid plasma and tissue turnover following absorption and tissue incorporation.

To resolve these gaps in knowledge, rats were administered the OXLAM, d4-13-hydroxyoctadecadienoic acid (d4-13-HODE) via gavage or intravenous (IV) injection, and the kinetics of its absorption and incorporation into adipose, liver, heart and brain were evaluated following optimization of the extraction and analytical procedures with Ultra High Performance Liquid Chromatography coupled to tandem mass spectrometry (UPLC-MS/MS). D4-13-HODE was administered in its unesterified (UE) form, to determine its distribution into UE and esterified (ES; i.e. lipoprotein-bound) plasma lipid pools following IV or gavage. We focused on 13-HODE, because it is the most abundant OXLAM in dietary oils, and in various tissues, including the brain [17,18,26]. Due to prior studies showing that dietary OXLAMs do not alter blood and tissue OXLAM concentrations [9,16], we hypothesized that d4-13-HODE would have limited bioavailability and rapid metabolism.

Contrary to the hypothesis, we found that free (i.e. UE) d4-13-HODE was absorbed following gavage, and that it incorporated into liver, heart and adipose, but not brain. Most of the IV-injected tracer remained UE in plasma post-injection, and most of the gavaged free tracer was recovered in plasma ES lipid pools. We therefore calculated tissue incorporation and turnover of the UE and ES tracer from IV-injected and gavaged rats, respectively, and found that tissues preferentially uptake ES over UE d4-13-HODE. Further, mass-spectrometry analysis revealed no downstream conversion into ketone- and tri-hydroxylated metabolites that serve as precursors to aldehydes [27].

2. Materials and methods

Unesterified d4-13(*S*)-HODE (d4-13S-hydroxy-9Z,11E-octadecadienoic-9,10,12,13 acid) was purchased from Cayman Chemicals (Catalog No. 338610, Ann Arbor, Michigan, USA). HEPES buffer was from Teknova (Cat No. H1030, Hollister, CA, USA). Fatty acid free Bovine Serum Albumin (BSA) Fraction V was from MP Biochemicals (Cat No. 0215240105, Solon, OH, USA), and sterile saline was from Spectrum Chemical (Cat No. S1941, New Brunswick, NJ, USA). Polypropylene Heparin-Lithium-Fluoride coated tubes were obtained from Beckman Coulter (Cat No. 6528824, Indianapolis, IN, USA).

2.1. Animal procedures

All procedures were performed in accordance with the guidelines of the National Institutes of Health Guide for the Care and Use of Laboratory Animals and were approved by the University of California Davis Institutional Animal Care and Use Committee (protocol # 19519, 21420 and 20541).

Male Fischer CDF rats weighing 200–220 g (~11.5 weeks of age; $n = 8$) with femoral vein vascular catheterizations were obtained from Charles River (Wilmington, MA, USA) and housed in a temperature and humidity controlled vivarium for two days. Food and water were provided ad libitum. The rats were maintained on the same Charles River diet (LabDiet 5L79, catalog number: 11000112) upon arrival. The diet contained 18% crude protein, 5% crude fat, 5% crude fiber, 8% ash, 12% moisture, 0.65% sodium, and 51.35% carbohydrate.

Rats were administered vehicle or d4-13-HODE via gavage or IV injection. The vehicle contained 5 mM HEPES buffer mixed with 50 mg/mL fatty acid free BSA. The UE-d4-13-HODE mixture contained 5 mM HEPES buffer, 50 mg/mL fatty acid free BSA and 0.22 mg/mL d4-13-HODE. Both vehicle and d4-13-HODE solutions were sonicated for 15 min. The solutions were mixed the day of or day prior to the experiment. If mixed the day prior, they were stored at −80 °C and thawed on ice prior to use. All solutions were kept on ice throughout the experiment and were thoroughly vortexed prior to being administered to the rats.

All rats were weighed prior to injection to determine tracer volumes. Eight rats were administered the following treatments: vehicle via gavage ($n = 1$), vehicle via intravenous (IV) injection (n = 1), d4-13-HODE via gavage ($n = 3$) or d4-13-HODE via IV (n = 3). The vehicle-injected rats served as negative controls ensuring the absence of tracer background during mass spectrometry analysis. The d4-13-HODE dose was 0.5 mg/kg per rat for both gavage and IV injection groups. This dose was based on a study showing bioactivity of another omega-6 fatty acid-derived lipid mediator, prostaglandin E2 (PGE2), when provided IV at 0.5 mg/kg [28]. The gavage and injection volumes ranged between 0.4 and 0.5 mL.

Blood was collected via tail vein or the femoral vein catheter from each rat at baseline (time 0, before tracer injection), and at 1, 3, 5, 10, 20, 30, 45, 60 and 90 min following vehicle or tracer administration, into Beckman Coulter polypropylene Heparin-Lithium-Fluoride coated tubes. The catheters were flushed with 0.1 to 0.2 ml sterile saline (0.9%) prior to and after blood collection. Following the final blood collection at 90 min, the rats were euthanized with CO_2 for approximately 2.5 min, decapitated and truncal blood collected at approximately 93–95 min. Blood was kept on ice and centrifuged at 15,871*g on an Eppendorf 5425 centrifuge (Hauppauge, NY, USA) for one minute to separate plasma. The separated plasma was transferred to new Beckman Coulter polypropylene Heparin-Lithium-Fluoride coated tubes and placed on dry ice. All tubes were stored in a -80 °C freezer until further analysis.

After euthanasia, the following tissues were dissected from each animal: right and left cerebrum, cerebellum, brainstem, heart, liver, lungs, stomach, small and large intestines, cecum, right and left kidney, lung and visceral and perirenal adipose, testis, skin and hind limb muscle. All tissues were obtained within 30 min after decapitation starting with the brain, and immediately flash-frozen in liquid nitrogen before being transferred to dry ice and storage at −80 °C. The analysis (below) was confined to adipose, liver, heart and brain. Other tissues remain stored in our freezer.

All animal procedures were completed within two consecutive days (8 rats on day 1 and 2 rats on day 2). One IV injected vehicle, one gavgaed vehicle, two IV injected and two gavaged tracer rats were completed on day 1; one IV injected and one gavaged tracer rats were completed on day 2.

Plasma and tissues were obtained from a separate group of Sprague-Dawley timed-pregnant female rats (Charles River Laboratories, Hollister, CA, USA) for method optimization of labeled and unlabeled 13-HODE measurements (n=4). Rats were individually housed on a 12:12 h light: dark cycle at ~22 °C with food and water available ad libitum. Blood and tissue collections were made following delivery of pups. Briefly, dams were deeply anesthetized with 4% isoflurane in oxygen. Blood samples were then collected via cardiac puncture. Blood was centrifuged 12,000*g for 10 min at 4 °C to obtain serum. For tissue collection, dams were euthanized via CO_2 asphyxiation followed by

cervical dislocation. Brain, heart, lung, liver, and visceral adipose tissues were collected and snap frozen in liquid nitrogen. All samples were stored at −80 °C. The method optimization was done on plasma and brain only.

2.2. Method optimization

Typically, total (i.e. UE + ES) oxylipins in plasma and tissues are measured following base hydrolysis, to liberate esterified oxylipins. However, both sodium carbonate (Na_2CO_3) and sodium hydroxide (NaOH) have been used at different concentrations and volumes to liberate esterified oxylipins [17,29,30]. Therefore, these bases were compared at different volumes and concentrations following extraction of total lipids from plasma, and from brain as a representative tissue, prior to measuring d4-13-HODE in the IV and gavaged rats.

Pooled plasma (1700 μL) was thawed on ice and 100 μL (n=4 per base treatment condition; see below) were transferred to 8 mL Kimble glass tubes containing 500 μL 1 mM ethylenediaminetetraacetic acid (EDTA) disodium salt dihydrate (Cat No. E5134, Sigma-Aldrich, St. Louis, MO, USA) and 0.9% NaCl (Cat No. S7653, Sigma-Aldrich, St. Louis, MO, USA) in milliQ water. Then, 2.4 mL of 2:1 (v/v) chloroform (Cat No. C607-4, Fisher Scientific, Hampton, NH, USA): methanol (Cat No. A454-4, Fisher Scientific, Hampton, NH, USA) containing 0.002% butylated hydroxytoluene (BHT, Cat No. W218405-SAMPLE-K, Sigma-Aldrich, St. Louis, MO, USA) was added. Samples were vortexed and centrifuged at 458*g for 10 min (Beckman Coulter Allegra 6 centrifuge, Indianapolis, IN, USA). The bottom chloroform layer was transferred to new tubes. 1.6 mL chloroform was added to the Kimble tubes, and the samples were vortexed, centrifuged and the second chloroform bottom layer was combined with first and evaporated under nitrogen.

The evaporated extract was reconstituted in 200 μL methanol containing 0.1% acetic acid (Cat No. 695092, Sigma-Aldrich St. Louis, MO, USA) and 0.1% BHT, 10 μL antioxidant (composition below), and spiked with 10 μL surrogate standard mix containing 2 μM d11–11(12)-EpETrE (Cat No. 10006413, Cayman Chemical, Ann Arbor, MI, USA), d11-14,15-DiHETrE (Cat No. 1008040, Cayman Chemical), d4-6-keto-PGF1α (Cat No. 315210, Cayman Chemical), d4-9-HODE (Cat No. 338410, Cayman Chemical), d4-LTB4 (Cat No. 320110, Cayman Chemical), d4-PGE2 (Cat No. 314010, Cayman Chemical), d4-TXB2 (Cat No. 319030, Cayman Chemical), d6-20-HETE (Cat No. 390030, Cayman Chemical) and d8-5-HETE (Cat No. 334230, Cayman Chemical). The antioxidant mix was made by mixing 0.2 mg/mL BHT, EDTA (Cat No. EDS-100G, Sigma-Aldrich, St. Louis, MO, USA) and triphenylphosphine (TPP, Cat No.3T84409 Sigma-Aldrich, St. Louis, MO, USA) in methanol/water (50/50, v/v)) and filtering the contents through 0.45 μm Millipore filter (Millpore, Bedford, MA, USA, cat No. SLHVM25NS).

The sample was hydrolyzed in 200 μL or 300 μL of 0.25 M NaOH (Cat No. S5881-500G, Sigma-Aldrich, St. Louis, MO, USA), 0.4 M NaOH or 0.25 M Na_2CO_3 (Cat No. 791768-500G, Sigma-Aldrich, St. Louis, MO, USA) in Methanol: MilliQ water (50/50 v/v; $n = 4$ per base treatment). Samples were vortexed and heated at 60 °C for 30 min, and cooled at room temperature for approximately 5 min. Then, 25 μL and 37.5 μL acetic acid were added to the tubes containing 200 μL and 300 μL base volumes, respectively, to bring the pH to 4–6 (verified on one sample by litmus paper). 1575 μL MilliQ water was added to samples that were hydrolyzed in 200 μL base and 1796 μL was added to samples that were hydrolyzed in 300 μL of base.

The hydrolyzed samples were loaded onto solid phase extraction (SPE) columns (Cat No. WAT094226, 60 mg Oasis HLB, Waters, Milford, MA, USA) pre-washed with one column volume of ethyl acetate (Cat No. E196-4, Fisher Scientific, Hampton, NH, USA) and two column volumes of methanol, and conditioned with two column volumes of SPE buffer (0.1% acetic acid, 5% methanol in ultrapure water). Samples were loaded onto the SPE columns, washed with two column volumes of SPE buffer and dried under vacuum for 20 min. Oxylipins were eluted with 0.5 mL methanol and 1.5 mL ethyl acetate. The eluent was dried under nitrogen, reconstituted in 50 μL LC-MS grade methanol (Cat No. A956, Fisher Scientific, Hampton, NH, USA), vortexed and centrifuged on Eppendorf 5424R centrifuge at 15,871*g (0 °C) for 2 min. The sample was transferred to centrifugal filter units (Cat No. UFC30VV00, Ultrafree-MC VV Centrifugal filters, Burlington, MA, USA) which were centrifuged at 15,871*g (0 °C) for 20 min. Samples were analyzed with UPLC-MS/MS as described below.

For optimization of the hydrolysis method on brain, a half cerebrum weighing ~845 mg was homogenized in ~845 μL 0.9% NaCl containing 1 mM EDTA disodium salt dihydrate in 2 mL centrifuge tube (Cat No. 1620-2700, USA scientific, Ocala, Florida, USA) using a bead homogenizer (Cat No. BBY24M Bullet Blender Storm, Next Advance, Troy, NY 12180, USA). The entire brain homogenate (~1.5 mL) was transferred to Kimble glass test-tubes containing 4 mL chloroform. The 2 mL centrifuge tubes were rinsed with 2 mL of methanol containing 0.006% BHT, vortexed and transferred to the 8 mL glass tubes containing chloroform (thus diluting the BHT content to 0.002%). Samples were vortexed and centrifuged at 920*g for 15 min at 0 °C. The bottom layer was pipetted to a clean test-tube. Lipids were re-extracted from the original sample with an additional 4 mL chloroform. The chloroform layers were pooled, evaporated under nitrogen and reconstituted in 5 mL of 2:1 v/v chloroform: isopropanol (Cat No. A464–1, Fisher Scientific, Hampton, NH, USA).

A portion of chloroform: isopropanol corresponding to 1 mg total lipid (based on an estimated 10% total lipid content per brain [31]) was hydrolyzed in 200 μL 0.25 M Na_2CO_3, 200 μL 0.4 M NaOH or 300 μL 0.4 M NaOH ($n = 4$ per treatment) at 60 °C for 30 min. The samples were cooled, acidified with acetic acid, diluted in water and purified with SPE and centrifugal filtering as described above for plasma, prior to UPLC-MS/MS analysis.

Standard recovery was determined for plasma and brain. The surrogate standard recovery was determined by dividing the peak area of surrogate in the sample post Folch extraction and hydrolysis, by the peak area of an equimolar surrogate standard mix that has not been subjected to Folch extraction and hydrolysis. Ion suppression was measured in brain extracts by pooling 15 μL from each base condition ($n = 4$ per condition; total volume = 60 μL), transferring two 20 μL aliquots of the sample mixture to new LC-MS vials, adding 30 μL of an oxylipin standard mix to one, and 30 μL methanol to the other (total volume = 50 μL per vial). Ten μL were injected into the UPLC-MS/MS, alongside 30 μL of the oxylipin standard mix diluted to the same level with 20 μL methanol. Percent ion suppression was calculated as follows: Peak area in spiked sample / (peak area in unspiked sample + peak area in standard mix) x 100.

2.3. Extraction of plasma and tissue from gavaged and IV injected rats

As described in the Results section, hydrolysis with 300 μL of 0.4 M NaOH yielded the best results, so we used it for measuring total oxylipins in plasma and tissue samples from the gavaged and IV injected rats (using the protocol described in Section 2.2).

For plasma, free and total oxylipins were extracted on the same day. Total oxylipins were extracted from 100 μL plasma and the remainder (3–100 μL) was used to isolate free oxylipins.

For free oxylipins, 200 μL extraction solvent, 10 μL antioxidant mix and 10 μL of 2 μM surrogate standard mixture were added to each plasma sample. Samples were vortexed and centrifuged at 21130*g at 0 °C for 15 min. The supernatant layer was transferred and MilliQ water (1113–1210 mL, depending on the plasma volume used) was added to each sample to achieve 15% methanol content. Samples were extracted with Oasis HLB columns as described above. Total oxylipins were extracted from plasma with the Folch method, hydrolyzed with 300 μL of 0.4 M NaOH (at 60 °C for 30 min) and subjected to SPE as described above.

Cerebrum (right side; 672 ± 36 mg), heart (663 ± 15 mg), liver (759 ± 177 mg), visceral adipose (189 ± 113 mg) and peri-renal adipose

(156 ± 63 mg) were extracted by the Folch method. For brain and liver, samples were homogenized in equal volumes of 0.9% NaCl containing 1 mM EDTA disodium salt dihydrate in 2 mL centrifuge tubes using a bead homogenizer. The homogenates were transferred to 8 mL glass tube containing 0.002% BHT in 5 mL chloroform: methanol (v/v: 2/1). 1 mL of chloroform/methanol was used to wash samples remaining in the 2 mL centrifuge tubes. The samples were vortexed, centrifuged at 920*g for 15 min at 0 °C and the bottom chloroform layer transferred to a new test-tube. Lipids were re-extracted by adding chloroform (4 mL) to the sample and pooling the second extract with the first.

For heart, samples were homogenized in equal volume of 0.9% NaCl containing 1 mM EDTA disodium salt dihydrate in 2 mL centrifuge tubes using a bead homogenizer. However, due to incomplete homogenization, the samples were transferred to 2 mL centrifuge tube containing 1 mL chloroform: methanol (v/v: 2/1) with 0.002% BHT, and further homogenized on a GenoGrinder 2010 (Spex, Metuchen, NJ) for 3 min at 1200 rpm and then for 13 min at 1400 rpm. The mixture was transferred to 8 mL glass tube containing 4 mL chloroform: methanol (v/v: 2/1) with 0.002% BHT. Another 1 mL was used to rinse the tubes. Samples were re-extracted with 4 mL of chloroform.

Visceral adipose was homogenized in 1.5 mL screw cap tubes (Cat No. TUBE1R5-S, Next Advance, Troy, NY 12180, USA) containing 1 mL 0.9% NaCl and 1 mM EDTA disodium salt dihydrate, using the bead homogenizer. The homogenates were transferred to Kimble test-tubes containing 5 mL chloroform/methanol with BHT; 1 mL of the chloroform/methanol/BHT mix was used to rinse the centrifuge tubes and the remaining extract was pooled with the other 5 mL in the Kimble tubes, for a total of 6 mL solvent. Then, 0.5 mL 0.9% NaCl containing 1 mM EDTA was added to the Kimble tubes. The samples were vortexed, centrifuged and re-extracted in 4 mL chloroform as described above for the other tissues.

For perirenal adipose tissue, the samples were also homogenized in 1.5 mL 0.9% NaCl containing 1 mM EDTA disodium salt dihydrate in 2 mL centrifuge tubes with a cap. However, the caps opened during homogenization for all three rats given the tracer via IV and one rat given the tracer via gavage. We attempted to recover the remaining homogenate by adding 1.5 mL of 0.9% NaCl containing 1 mM EDTA disodium salt dihydrate, vortexing and transferring the homogenate to Kimble test-tubes containing 4 mL of chloroform/methanol with 0.002% BHT. 1 mL of the chloroform/methanol/BHT mix was used to rinse the centrifuge tube twice (total of 2 mL). The samples were vortexed, centrifuged and re-extracted in 4 mL chloroform. The extraction proceeded as described above for visceral adipose tissue. Samples that were not lost during homogenization were transferred to Kimble glass-tubes containing chloroform/methanol/BHT; 1 mL was used to rinse the tubes twice and the extracts were pooled. The samples were re-extracted with 4 mL chloroform.

For all tissues, a portion of the total lipid extract amounting to ~3 mg lipid per tissue was reconstituted in 200 μL extraction solvent and hydrolyzed in 300 μL 0.4 M NaOH. Acetic acid and water were added and the oxylipins extracted with SPE as described above.

2.4. UPLC-MS/MS analysis

Samples were analyzed on an Agilent 1290 Infinity UPLC system connected to an Agilent 6460 triple-quadrupole tandem mass spectrometer (Agilent, Palo Alto, CA, USA) equipped with a Jetstream electrospray ionization source as previously detailed [14,32]. Unlabeled oxylipins were analyzed in negative ionization mode and probed using published optimized dynamic Multiple Reaction Monitoring conditions [14,32]. The optimized transition for d4-13-HODE was 299.3–198.1, which was consistent with the literature [33]. We also probed for labeled downstream metabolites of d4-13-HODE in tissues, specifically d3-13-oxo-ODE (296.2–198.1) and d4-9,10,13-TriHOME (333.2–172.1/171.1). The collision energy for all labeled compounds was 10 V.

Analytes were separated with reverse phase liquid chromatography, using an Agilent Eclipse Plus C18 column (2.1 × 150 mm, 1.8 μm Agilent Corporation). The auto-sampler temperature was set at 4 °C and the column temperature was set at 45 °C. The same mobile phases and conditions published previously were used. In brief, mobile phase A had 0.1% acetic acid in ultrapure water and mobile phase B had 80/15 acetonitrile/methanol (v/v) with 0.1% acetic acid [14,32]. Mobile phase A was initially at 65%. It was decreased to 60% at 3 min, 52% at 4 min, 40% at 10 min, 30% at 20 min, 15% at 24 min and 0% by 24.6 min. Mobile phase B was therefore at 100% at 24.6 min and held there to 26.1 min. Mobile phase A was increased to 65% at 26.10 min and held constant to 27.30 min for the remainder of the run, which ended at 28 min. The flow rate was 0.3 mL/min between 0 to 3 min, 0.25 mL/min from 3 to 24.5 min, 0.35 mL/min from 24.6 to 27.0 mins, and 0.30 mL/min from 27.3 to 28 min.

Samples that utilized d4-PGE2 as a surrogate standard were not quantified because it degrades during hydrolysis. These include LA-derived trihydroxylated metabolites (9,10,13-TriHOME and 9,12,13-TriHOME) and prostaglandins (PGB2, PGD1, PGD2, PGD3, PGE1, PGE2, PGE3, 15-deoxy-PGJ2 and PFG2-alpha).

2.5. Kinetics

The volume of distribution (V_d) of the injected UE d4-13-HODE tracer was calculated as follows:

$$V_d = D/C_{UE} \tag{1}$$

where D is the dose of the injected tracer and C_{UE} is the peak plasma concentration of UE d4-13-HODE following injection (i.e. at 1 min).

Plasma half-life of UE d4-13-HODE was derived from the plasma curve of IV-injected rats by taking the first derivative of plasma concentration, starting at 1 min, the time at which injected d4-13-HODE concentration reached peak values, to 5 min, when the tracer appeared to plateau between the non-detectable to 1 pmol/μL range. Thus, the rate of UE tracer elimination was determined using Eq. (2) below. A similar calculation was used to determine the rate of total d4-13-HODE tracer elimination, by measuring the rate of total d4-13-HODE disappearance between 1 to 5 min following IV injection.

$$Rate\ of\ tracer\ elimination(R) = \frac{dC^*_{UE}}{dt(1-5min)} \tag{2}$$

where C* is d4-13-HODE concentration in plasma, t is time, and k^* is the slope constant. Zero order and first order kinetic plots were generated to determine the plot that generated a linear relationship. As shown in Supplement Fig. 1, plotting the natural log of C versus time for UE or total d4-13-HODE resulted in a linear slope with an R^2 of 0.9749 and 0.9875, respectively, suggesting first order kinetics. The slope of the line (i.e. the k^* value) was used to calculate the half-life of the free, injected d4-13-HODE as follows:

$$Plasma\ UE\ t_{1/2} = \frac{ln2}{slope\ (k^*)} \tag{3}$$

The rate of ES d4-13-HODE incorporation into plasma following gavage was determined by taking the first derivative of the tracer concentration versus time plot, and re-plotting that against time. Because negligible d4-13-HODE was found in the free pool, the total amount in plasma after gavage represents the ES pool. Thus,

$$Plasma\ J_{in\ (ES)} = \frac{dC^*_{total}}{dt_{0\ to\ 90\ min}} \tag{4}$$

The maximum rate of incorporation, $J_{in\ (ES)}$, representing maximum velocity of incorporation was derived from the maximum point on the dC/dt versus time plot. This was then used to calculate turnover (F) of esterified d4-13-HODE as follows,

$$Plasma\ F_{ES} = \frac{Jin_{ES}}{C_{total}} \quad (5)$$

Here, C_{total} is the unlabeled total 13-HODE concentration at the maximum velocity of incorporation, based on Eq. (4) (i.e. at $J_{in(ES)}$)

The half-life of the esterified 13-HODE was determined as follows,

$$Plasma\ ES\ t_{1/2} = \frac{ln2}{F_{ES}} \quad (6)$$

The plasma area under the curve (AUC) was determined by trapezoid integration of the plasma total and free d4-13-HODE concentration from 0 to 90 min, following IV or gavage. The incorporation coefficient of UE d4-13-HODE, k^*_{UE}, for each tissue, was calculated as follows,

$$Tissue\ k^*_{UE} = \text{Tracer tissue concentration}_{\text{Total}} / \text{AUC}_{\text{UE}} \quad (7)$$

where tracer tissue concentration$_{Total}$ represents the sum of ES and UE tracer in each tissue, because only total d4-13-HODE was measured. The AUC_{UE} is derived from the IV-injected rats.

The incorporation rate (J_{in}) of UE d4-13-HODE into tissues was determined as follows,

$$Tissue\ J_{in}(UE) = k^*_{UE} x C_{UE\ plasma} \quad (8)$$

where C_{UE} plasma is the concentration of free, unlabeled 13-HODE in plasma at 90 min or 95 min (from sample collected after decapitation) depending on availability. For one of the rats, we used UE concentration at 30 min, due to insufficient plasma volume at other time-points following tracer measurements.

Turnover, representing the rate of UE tracer replacing endogenous 13-HODE within tissues was calculated according the following equation,

$$Tissue\ F_{total} = \frac{J_{in} UE}{C_{total}} \quad (9)$$

where C_{total} is the total (UE + ES), unlabeled amount of 13-HODE in tissues. Tracer half-life ($t_{1/2}$) within tissues was determined using Eq. (6), where ln2 is divided by tissue turnover (*F*) calculated in Eq. (9).

To determine the contribution of ES d4-13-HODE incorporation from plasma into tissues, we integrated the following equation [34],

The rate of tissue incorporation is,

$$\frac{dC^*tissue}{dt} = k^*_{UE} C^*_{plasma(UE)} + k^*_{ES} C^*_{plasma(ES)} \quad (10)$$

The integral yielded the equation below, where k^*_{UE} is derived from the IV-injected rats using Eq. (7) above.

$$C^*_{tissue}(T) = k^*_{UE} \int_0^T C^*plasma(UE)dt + k^*_{ES} \int_0^T C^*plasma(ES)dt \quad (11)$$

Eq. (11) was solved for k^*_{ES}, which is the incorporation coefficient for esterified d4-13-HODE in tissues. This was calculated because we did not inject ES d4-13-HODE. Notably, a similar k^*_{ES} value can be derived from the quotient of tissue total d4-13-HODE concentration and the AUC for ES d4-13-HODE, determined by subtracting the AUC of free d4-13-HODE from the AUC of total d4-13-HODE. The incorporation rate of esterified d4-13-HODE, $J_{in(ES)}$, into tissues was then calculated as follows,

$$Tissue\ J_{in}(ES) = k^*_{ES} x C_{ES\ plasma} \quad (12)$$

where C_{ES} plasma is the amount of unlabeled, esterified 13-HODE in plasma at 90 min or 95 min depending on plasma availability. The 95 min plasma time-point was collected after decapitation. C_{ES} plasma was calculated by subtracting free 13-HODE from total 13-HODE.

2.6. Statistical analysis

The sample size justification for 3 rats per route of administration for d4-13-HODE was based on similar studies which used a sample size of 3 to 4, to examine the metabolism of labeled oxylipins (e.g. PGE2 or LNA-hydroperoxide) in rats [25,35,36]. Data were analyzed on GraphPad Prism version 8.4.3 (GraphPad Software, San Diego, California USA), and expressed as mean ± standard deviation (SD). One-way analysis of variance (ANOVA) followed by Tukey's post-hoc test was used to compare across methods. An unpaired *t*-test was used to compare log-transformed values for labeled and unlabeled 13-HODE concentrations and kinetics in tissues and plasma because analysis by Shapiro–Wilk's test showed that the data were not normally distributed. Body weight and heart weight were also not normally distributed, so an unpaired t-test on log-transformed values was applied. To maintain statistical consistency, the same t-test was applied on log-transformed data of liver, cerebrum and adipose (despite being normally distributed). A $P < 0.05$ was considered statistically significant.

3. Results

3.1. Base hydrolysis method

The hydrolysis efficiency of 200 and 300 μL of NaOH or Na_2CO_3, at 0.25 M and 0.4 M each, was tested on 100 μL rat plasma. As shown in Supplement Table 1, 300 μL 0.4 M NaOH yielded the highest concentration of oxylipins with the lowest SDs. Surrogate recoveries (Supplement Table 2) were similar across the different base conditions, and did not statistically differ from each other. As expected, d4-PGE2 was lost during hydrolysis with both bases.

The hydrolysis efficiency of 200 μL of 0.25 M Na_2CO_3, 200 μL of 0.4 M NaOH, and 300 μL of 0.4 M NaOH was tested on rat brain tissue lipid extracts. As shown in Supplement Table 3, 300 μL of 0.4 M NaOH yielded the highest concentration of oxylipins. Surrogate recoveries were similar across the various base treatments (Supplement Table 4). Ion suppression was minimal for the majority of compounds across the three base treatments as shown in Supplement Table 5.

Based on the above findings, 300 μL of 0.4 M NaOH was used on plasma and tissues (below), because it yielded the highest concentration of oxylipins.

3.2. Body and organ weights

Body and organ weights did not differ significantly between the gavage and IV groups ($P > 0.05$ by unpaired *t*-test on log-transformed values; $n = 4$ per group including the rats gavaged or injected with vehicle). Rats in the gavage and IV-injected groups weighed 195 ± 9 g and 178 ± 49 g, respectively. At the time of sacrifice, cerebrum weighed 0.7 ± 0.04 g and 0.7 ± 0.03 g, peri-renal adipose was 0.2 ± 0.1 g and 0.2 ± 0.1 g, visceral adipose was 0.2 ± 0.1 g and 0.2 ± 0.1 g, heart was 0.7 ± 0.02 g and 0.5 ± 0.3 g and liver was 0.9 ± 0.1 g and 0.7 ± 0.2 g in the gavaged and IV-injected rats, respectively.

3.3. Volume of distribution

The volume of distribution, derived from peak UE d4-13-HODE concentration at 1 min following IV injection was 102.35 mL (n=1, since plasma for UE tracer quantitation was available at 1 min from one rat; see Section 3.4). This value is 8-fold greater than the reported blood volume of 12.7 mL for rats at this age [37], suggesting that the injected tracer likely went into tissues.

3.4. Plasma tracer incorporation after IV injection and gavage

Fig. 1-A and B show mean UE and total (i.e. UE+ES) d4 13-HODE concentrations over the 90-min monitoring period following IV and gavage administration of the tracer, respectively. There were multiple missing values for UE d4 13-HODE measured in both gavage- and IV-treated rats, due to the lack of sufficient sample volume at several time-

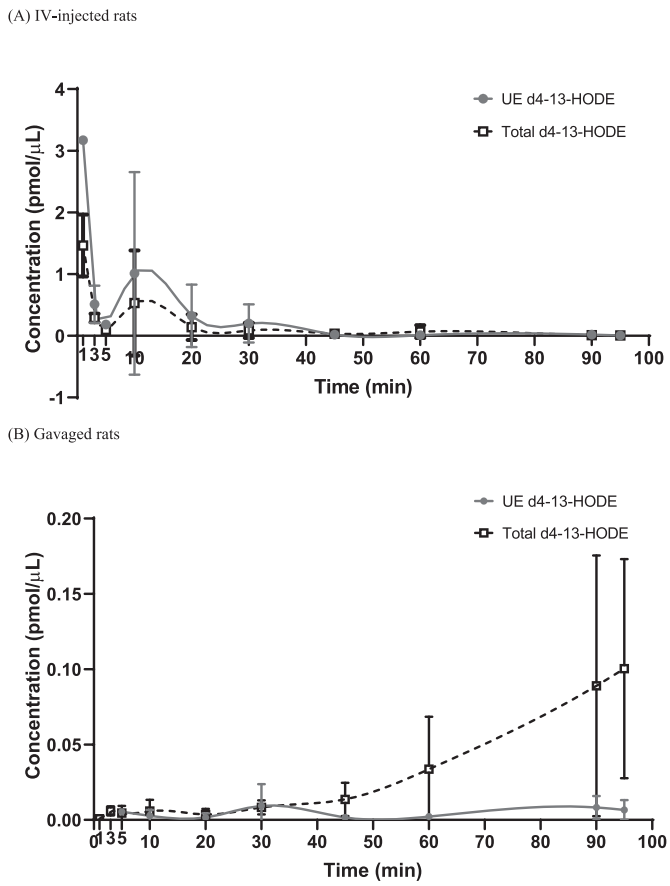

Fig. 1. Concentration-Time plot of d4-13-HODE in plasma of rats injected IV (A) or gavaged (B) with the tracer. For (A), data are mean ± SD of $n = 3$ per group for total d4-13-HODE, and $n = 2$–3 for unesterified (UE) d4-13-HODE, except at one min where $n = 1$. For (B), data are mean ± SD of n = 3 per group for total d4-13-HODE, except at 3, 10 and 45 min where $n = 2$. Data are 2–3 per time-point for UE d4-13-HODE, except at 1 min (n = 1), and at 3 and 5 min, where we did not have sufficient plasma volume left in all 3 rats for free tracer measurements.

points. Hence, data were available from 2 to 3 rats per time-point, except for the 1 min time-point in the IV-injected group, where only one sample could be assayed. Error bars (i.e. SDs) are shown when the sample size is 2 to 3. Individual Concentration-Time plots for UE and total d4 13-HODE of each rat are presented in Supplement Fig. 2.

No tracer was detected in plasma at any time-point in vehicle-treated rats ($n = 1$ gavage and n = 1 IV). UE and total (UE + ES) d4-13-HODE were detected in plasma of gavage- and IV- treated rats ($n = 3$ per treatment). As shown in Fig. 1-A, after IV tracer injection, the concentration of UE d4-13-HODE was highest at 1 min (3.17 pmol/μL), and dropped rapidly to 0.18 pmol/μL within 3 min, and to negligible levels by 40 min. Total d4-13-HODE was lower in concentration by approximately 2-fold relative to UE d4-13-HODE during the first 30 min, likely due to d4-13-HODE losses during SPE or degradation during base hydrolysis, as previously reported [30]. The fact that the majority of the tracer was recovered in the free pool, suggests that the injected tracer did not incorporate into ES lipids. This is also supported by the observation that total d4-13-HODE elimination pattern mirrored that of the free pool (Fig. 1-A).

In gavaged rats (Fig. 1-B), the majority of d4-13-HODE in plasma was found in the total pool. It was detected there from 3 to 20 min after gavage at a low concentration of approximately 0.0059 pmol/μL. This concentration gradually increased after 20 min and reached 0.10 pmol/μL by 90 min. UE d4-13-HODE was detected at 5 min (0.0054 pmol/μL) following gavage, and remained relatively low during the 90 min sampling period (range of 0.0016–0.0093 pmol/μL). UE d4-13-HODE constituted 48.2% of the total d4-13-HODE pool at the beginning (between 0 and 10 min), and 2.0% of the total pool between 45 and 60 min, suggesting that the majority of the gavaged tracer incorporated into esterified plasma lipid pools over time.

Plasma unlabeled 13-HODE concentrations (UE and total) were relatively stable over time (Supplement Fig. 3-A&B), suggesting that the injected or gavaged tracer did not alter endogenous pools.

3.5. Plasma AUC after tracer IV injection and gavage

In IV-injected rats, the AUC was 16.4 ± 19.3 pmol*min/μL for free d4-13-HODE and 11.7 ± 12.1 mol*min/μL for total d4-13-HODE ($P > 0.05$ by unpaired *t*-test on log-transformed values). The AUC was 0.3 ± 0.2 and 2.4 ± 1.9 pmol*min/μL for free and total d4-13-HODE, respectively, in the group that received the tracer via gavage ($P < 0.05$ by unpaired t-test on log-transformed values).

3.6. Plasma kinetics after IV injection and gavage

Plasma total d4-13-HODE kinetics following IV or gavage are reported in Table 1. Because all free tracer was found in the total pool after IV injection, it can be assumed that total d4-13-HODE elimination kinetics represent the elimination of UE d4-13-HODE. Similarly, total d4-13-HODE plasma incorporation kinetics reflect ES d4-13-HODE kinetics in the gavage rats, since most of the tracer was found in ES fractions.

The rate constant for elimination (k^*) of the injected UE d4-13-HODE was higher (by 42-fold) than the rate constant (F) for incorporation into plasma following gavage. This is in agreement with the greater elimination rate (R_{max}) of the IV-injected tracer compared to incorporation rate (J_{in}) of the gavaged tracer.

The half-life of the injected d4-13-HODE was derived from the natural log-transformed concentration-time plot shown in Supplement Fig. 1. The half-life of total d4-13-HODE following IV injection was approximately 1 min (61.3 ± 9.47 s, $n = 3$; Table 1). A similar half-half of 58.2 s was obtained for UE d4-13-HODE, although this was based on one rat where the UE tracer was measured at 1 min (we did not have sufficient plasma left in the other 2 rats to measure UE tracer concentrations at this time-point). Similarities between the total and free pool half-lives confirm that the majority of injected d4-13-HODE was in the free pool.

The half-life of the ES tracer was determined from the first derivative plots of concentration versus time following d4-13-HODE gavage (Supplement Fig. 4). Rats reached maximal incorporation rates (J_{in}) within 3–90 min. The calculated mean half-life was 71.2 min (Table 1).

3.7. Tissue total d4-13-HODE and unlabeled 13-HODE concentrations

Total (UE and ES) d4-13-HODE and endogenous (unlabeled) 13-HODE were measured in plasma, adipose, liver, heart and brain by UPLC-MS/MS. No peaks were observed in the vehicle-treated rats in all

Table 1
Kinetics of d4-13-HODE in plasma total (i.e. UE + ES fractions) following IV or gavage free d4-13-HODE administration.

	IV (n = 3)	Gavage (n = 3)
k^* *or* F (min^{-1})[a]	0.67 ± 0.10	0.016 ± 0.010
R_{max} or J_{in}[b] ((pmol/(uL×min))	−0.34 ± 0.13	0.0028 ± 0.0018
Half-life ($t_{1/2}$, min)	1.05 ± 0.16	71.19 ± 68.95

Data are mean ± SD of n = 3 per group. Data were not statistically compared because IV kinetics reflect tracer elimination and gavage kinetics reflect tracer incorporation. Data are presented as mean ± SD of n = 3 rats per group.

[a] k^* is the rate constant for UE 13-HODE; F is turnover for ES 13-HODE.

[b] R_{max} is the rate of UE d4-13-HODE elimination from plasma; J_{in} is the rate of ES d4-13-HODE incorporation into plasma following gavage.

tissues assayed (Supplement Fig. 5). Concentrations of total (UE + ES) labeled and unlabeled 13-HODE in tissues and plasma (collected after decapitation) of rats gavaged or injected IV with the tracer are reported in Table 2.

As shown in Table 2, d4-13-HODE was detected in visceral adipose, heart and liver following IV and gavage tracer administration. There were no significant differences in tracer concentrations in these tissues between the IV-injected versus gavage-treated rats. No tracer was detected in the brain after IV or gavage administration. D4-13-HODE was detected in perirenal adipose of IV-infused rats (chromatograms in Supplement Fig. 5-A) but as described in the Methods, due to sample loss, tracer concentrations were not quantifiable. D4-13-HODE was not detected in perirenal adipose of rats gavaged with the tracer, likely due to sample loss during the extraction (Supplement Fig. 5-A). Raw chromatograms for the remaining tissues, per rat, are in Supplement Fig. 5 (B to E). At the time of death, plasma total d4-13-HODE concentration was significantly higher in gavaged rats than IV-injected rats, consistent with the continued appearance of the tracer in plasma over time following gavage.

Unlabeled 13-HODE was observed in all tissues irrespective of tracer method of administration (Table 2). It was seen in peri-renal adipose, but again, quantitation was not possible due to accidental loss during homogenization. In visceral adipose, heart, liver and brain, no significant differences were seen in unlabeled 13-HODE concentration between IV and gavage treated rats.

Notably, unlabeled 13-HODE was most abundant in visceral and perirenal adipose tissue (10–27 pmol/mg), followed by heart (~1.5 pmol/mg), liver (~1.2 pmol/mg) and brain (~0.15 pmol/mg). This hierarchy was also reflected in tracer concentrations, where visceral adipose d4-13-HODE concentration was 30-353 and 92-546 fold higher than in heart and liver, respectively (none in brain). The variability, based on standard deviations, was higher for both unlabeled and labaled 13-HODE in metabolic tissues such as adipose and liver, compared to heart and brain.

3.8. Kinetics of d4-13-HODE

The incorporation coefficient (k_i^*), incorporation rate (J_{in}), turnover (F) and half-life ($t_{1/2}$) of UE and ES d4-13-HODE in adipose, liver and heart are reported in Table 3. AUC values used to derive the k_i^* values are also reported in Table 3. It should be noted that ES tracer kinetics were derived from the ES tracer AUC, determined from the difference between total and free AUC in gavaged rats. The gavaged rats were used to derive ES kinetics, because most of the tracer was esterified post-gavage. The IV-injected rats were used to derive UE incorporation into tissues, because most of the tracer was unesterified after IV injection.

Table 2
Total (UE + ES) labeled and unlabeled 13-HODE concentrations (pmol/mg or pmol/uL) in visceral and perirenal adipose, liver, heart, brain and plasma (after death). UE, Unesterified; ES, Esterified.

	d4-13-HODE concentration (pmol/mg)		Unlabeled 13-HODE concentration (pmol/mg)	
	IV	Gavage	IV	Gavage
Visceral adipose	0.33 ± 0.30	3.11 ± 5.00	16.49 ± 12.86	9.84 ± 5.60
Perirenal adipose	Detected but not quantified due to sample loss[1]	Not detected, likely due to sample loss[1]	Detected but not quantified due to sample loss[1]	26.86 ± 7.81
Liver	0.0036 ± 0.0029	0.0057 ± 0.0057	1.08 ± 0.38	1.22 ± 0.88
Heart	0.011 ± 0.001	0.0088 ± 0.0061	1.40 ± 0.40	1.56 ± 0.35
Brain	Not detected	Not detected	0.11 ± 0.03	0.18 ± 0.08
Plasma (after death)	0.004 ± 0.002	0.100 ± 0.073*	0.20 ± 0.05	0.13 ± 0.06

Data are mean ± SD of n = 3 per group. [1]Not quantifiable because the sample tube caps opened during homogenization, resulting in sample loss (as described in the methods section).
* $P < 0.05$ by unpaired t-test on log-transformed data, comparing gavage versus IV.

Table 3
AUC (pmol×min/μL), incorporation coefficient (K^*) (μL/(mg × min), incorporation rate, J_{in} ((pmol/(mg × min)), turnover, F (min^{-1}), half life, $t_{1/2}$ (min) in visceral adipose, liver, and heart in IV and gavage rats.

		IV (UE)	Gavage (ES)
Plasma d4-13-HODE AUC		16.4 ± 19.3	2.1 ± 1.7[1]
Visceral adipose	k^*	0.047 ± 0.041	0.88 ± 1.16
Liver	k^* ($\times 10^{-4}$)	3.6 ± 3.8	22.9 ± 12.2†
Heart	k^* ($\times 10^{-4}$)	20.3 ± 21.1	42.4 ± 23.0
Visceral adipose	J_{in} ($\times 10^{-4}$)	22.2 ± 17.1	846.2 ± 1250.0
Liver	J_{in} ($\times 10^{-4}$)	0.18 ± 0.15	1.9 ± 1.3†
Heart	J_{in} ($\times 10^{-4}$)	1.0 ± 1.0	3.2 ± 1.7
Visceral adipose	F ($\times 10^{-4}$)	1.6 ± 1.5	65.1 ± 72.3†
Liver	F ($\times 10^{-4}$)	0.15 ± 0.075	1.7 ± 1.1 ††
Heart	F ($\times 10^{-4}$)	0.7 ± 0.6	2.2 ± 1.5
Visceral adipose	$t_{1/2}$($\times 10^{4}$)	0.9 ± 0.9 (6.2 days)	0.05 ± 0.07 (0.34 day)†
Liver	$t_{1/2}$($\times 10^{4}$)	5.5 ± 2.3 (38.3 days)	0.5 ± 0.3 (3.6 days)††
Heart	$t_{1/2}$($\times 10^{4}$)	2.1 ± 2.3 (14.7 days)	0.4 ± 0.3 (3.1 days)

Data are mean ± SD of n = 3 per group. †Indicates significant differences in log-transformed values between IV and gavage groups, by unpaired t-test applied to log-transformed values. †P<0,05; ††P<0.01.
[1]*Ester*ified d4-13-HODE AUC determined by subtracting free from total d4-13-HODE AUC in each individual rat that received the tracer via gavage.

The incorporation coefficient, k_i^* in liver was significantly higher by 6-fold for ES d4-13-HODE compared to UE d4-13-HODE ($P < 0.05$). It was 19- and 2-fold higher for ES d4-13-HODE in visceral adipose and heart, but this change was not statistically significant.

The incorporation rate, J_{in}, into adipose, liver and heart was also higher by 38-, 11,- and 3-fold for ES versus UE d4-13-HODE, but changes were only statistically significant for liver ($P < 0.05$).

Turnover, F, was significantly higher for ES than UE tracer in adipose and liver by 40- and 11-fold, respectively. ES tracer turnover was 3 times higher than UE turnover in heart, but this difference was not statistically significant.

UE tracer half-life ranged from 6 to 36 days, whereas ES half-life ranged from 0.3 to 3.6 days in adipose, liver and heart. Thus, the half-life of the ES tracer in these tissues was 5–18 times shorter than the half-life of the UE tracer. Statistical significance in tracer half-life was only seen for visceral adipose and liver.

To confirm that a similar amount of free tracer were incorporated into tissues following IV or gavage tracer administration, we compared J_{in} (UE) into tissues (visceral adipose, liver and heart) following gavage, to *Jin* (UE) following IV. As shown in Supplement Table 6, no significant differences were observed, per tissue, suggesting that that the incorporation rate of the UE tracer into tissues was similar independent of the route of administration.

3.9. Metabolism of d4-13-HODE into other downstream metabolites in tissues

To test whether d4-13-HODE was converted into other downstream ketones or tri-hydroxylated metabolites, we probed for d3-13-oxo-ODE and d4-9,10,13-TriHOME in adipose (peri-renal and visceral), liver, heart and brain of IV and gavage rats. As shown in Supplement Fig. 6, no tracer was detected during the transition times for either metabolite in any of the tissues, irrespective of the mode of administration.

4. Discussion

This study demonstrates that LNA-derived 13-HODE is bioavailable

and that it rapidly incorporates into liver, heart and adipose, but not brain. Tracer incorporation into liver, heart and adipose from ES 13-HODE was faster compared to UE 13-HODE, suggesting that peripheral tissues preferentially uptake ES over free 13-HODE.

Although free OXLAM incorporation into peripheral tissues has been previously reported [38], this is the first study to quantitatively demonstrate that ES d4-13-HODE preferentially incorporates into peripheral tissues. Bergan and Draper [23] detected radioactivity in heart, liver and adipose but not brain after gavaging free ^{14}C-labeled LA hydroperoxides. Samuelsson et al. reported that tritiated PGE2 (a metabolite of arachidonic acid, ARA), also incorporated into liver, heart, adipose, and brain after IV infusion [35]. Although these studies suggest that free oxylipins enter tissues, the use of radiolabeled tracers do not inform on whether the intact tracer or a metabolite of the tracer incorporated into tissues. Mass-spectrometry analysis performed in this study ascertained that the intact d4-13-HODE tracer incorporated into peripheral tissues from plasma.

The plasma half-life of free (UE) d4-13-HODE was >70-fold lower than that of the bound (ES) tracer (~ 1 vs 71 min). The short half-life of the free tracer is consistent with its observed high volume of distribution (102 mL), relative to the average rat blood volume of 12.7 mL [37]. This means that upon inection, the free tracer preferentially incorporated into tissues, as confirmed in Table 3 (versus binding to plasma proteins). The longer plasma half-life of ES d4-13-HODE is comparable to the reported absorption half-life of esterified conjugated LNA of 20 to 32 min and reflects lipoprotein-mediated mechanisms of transport [39]. In contrast, UE 13-HODE likely non-covalently associates with albumin, similar to UE fatty acids [40], which means that elimination is dependent on rapid diffusion into tissues rather than lipoprotein-mediated receptor uptake (slower process) as is the case for ES lipids. The notably high variability in ES plasma half-life (coefficient of variation (CV) of 97%) compared to that of UE d4-13-HODE (CV of 15%) is likely due to postprandial differences in free d4-13-HODE absorption, since food was provided ad libitum. There is limited information on postprandial 13-HODE response in rodents, but in non-fasted humans, a high post-prandial variability in 13-HODE (CV of 40–70%) was reported [41]. Fasting the rats prior to tracer administration may reduce the variability in 13-HODE plasma metabolism, as reported in humans [42].

The incorporation coefficient, k^*, is a marker of tissue avidity towards the tracer [43,44]. In this study, k_{ES}^* was 2–19 fold higher than k_{UE}^* in visceral adipose, liver and heart, with statistical significance observed for liver only (Table 3), suggesting that these tissues preferentially uptake ES over UE 13-HODE. This does not imply that these tissues solely uptake the ES tracer; in fact, they showed affinity towards both the UE and ES tracer, but affinity was greater towards the lipoprotein-bound ES tracer (Table 3).

The incorporation rate, J_{in}, is a quantitative measure of the amount of tracer that incorporates from plasma into tissues, per unit time [45]. As shown in Table 3, both UE and ES tracers incorporated into adipose, liver and heart. However, the rate of ES d4-13-HODE incorporation into tissues was 3–38 fold greater than UE d4-13-HODE (significant for liver only). This is consistent with the significantly greater tissue affinity (k^*) towards ES than UE d4-13-HODE in liver.

Turnover, reflecting the rate at which the incorporated tracer replaces endogenous (unlabeled) 13-HODE pools lost during metabolism [46], was 3–40 times higher in adipose, liver and heart for ES d4-13-HODE than UE d4-13-HODE. Differences were statistically significant for adipose tissue and liver, and indicate rapid turnover of ES 13-HODE within these compartments. The turnover measurements are likely underestimated because they do not account for the rate of tracer acylation/deacylation within tissue lipid compartments [46]. Measuring labeled 13-HODE-CoA pools would provide a more complete picture of d4-13-HODE recycling within adipose, liver and heart.

We were not able to detect measurable loss into downstream products (ketone- and tri-hydroxy metabolites), although metabolism into other compounds not covered by our targeted UPLC-MS/MS platform is possible. Fang et al. reported that 13-HODE can be metabolized into 11-hydroxyhexadecadienoic acid, 9-hydroxytetradecadienoic acid, and 7-hydroxydodecadienoic acid, which were not measured in this study [47]. Additionally, a recent study showed that hydroxylated metabolites of docosahexaenoic acid undergo β-oxidation ex vivo, to form malic acid, butainetriol, and other short-chain hydroxy-fatty acids [48], raising the possibility that a similar oxidation pathway may exist for 13-HODE. Tissue release is also likely, particularly for adipose tissue, which has the highest concentration and turnover of ES 13-HODE compared to other tissues, consistent with its physiological role as a reservoir and supplier of oxylipins [49,50].

The low tissue turnover of UE 13-HODE compared to ES 13-HODE may be due to its rapid esterification upon entering tissues, resulting in 'trapping' of the tracer by peripheral tissues. If so, then the measured rates of incorporation of free d4-13-HODE (J_{inUE}) reflect actual esterification rates in vivo. We did not measure unlabeled tissue concentrations of free 13-HODE in this study, a limitation which prevents us from capturing turnover within the free pool. Free oxylipin concentrations are low in tissues, and increase dramatically during euthanasia due to postmortem ischemia [32]. Hence, this aspect of the study should be re-examined in rats subjected to high-energy microwave fixation [32].

Compared to fatty acids, the kinetics of UE 13-HODE are similar in plasma but different in tissues. For instance, the plasma half-life of free 13-HODE (~1 min) is comparable to that of ethyl LNA (39 s), palmitic acid (48 s) and docosahexaenoic acid (40s) in rats [40,51,52]. It is also comparable to the half-life of other UE oxylipins, including ARA-derived PGE2 and PGF1α in humans (<1.5 min) [53] and PGF2α in horses (94.2 s) and cows (29.2 s) [54]. The opposite is observed for tissues, however, where free 13-HODE incorporates slower than free fatty acids. For instance, heart UE palmitic acid, ARA and eicosapentaenoic Acid (EPA) k^* values of 0.11, 0.36 and 0.13 μL/(mg × min), respectively, are 55–180 times higher than our measured heart d4-13-HODE k_{UE}^* of 0.002 μL/(mg × min) (Table 3) [55,56]. Liver UE EPA k^* of 0.44 μL/(mg × min) is >1200-fold higher than d4-13-HODE k_{UE}^* value of 0.00036 μL/(mg × min) in liver [56]. Similarly, UE EPA incorporation rate into heart (0.86 pmol/(mg × min)) and liver (3.1 pmol/(mg × min)) is orders of magnitude higher than both UE and ES d4-13-HODE incorporation rates into these tissues [56]. Collectively, the evidence suggests that tissues incorporate free fatty acids preferentially and more rapidly compared to UE or ESally comp13-HODE.

The half-life of ES 13-HODE (71 min), is five times less than the half-life of its precursor, ES LNA (446 min) in plasma [57], and more than 50 fold smaller than the plasma half-life of ES ARA (2.2 to 27.6 days depending on the dietary content of LNA) [58], suggesting faster plasma clearance of ES 13-HODE compared to ES fatty acids. Once in tissues, however, ES 13-HODE appears to be utilized slower than fatty acids. Based on the turnover measurements, ES d4-13-HODE half-life of 3.1 and 3.6 days in heart and liver, respectively, is greater than the reported half-life of ES EPA in heart (2.7 h) and liver (4.6 h) [56]. These differences suggest that incorporated OXLAMs are likely to reside longer in tissues compared to fatty acids. Thus, overall, they incorporate slower and remain longer in tissues compared to fatty acids.

Schuster et al. reported that chronic (8 week) intake of dietary OXLAMs by mice did not increase plasma OXLAM concentrations, raising questions on their bioavailability [9]. The present study indicates that 13-HODE (an OXLAM) is indeed bioavailable. The kinetic data suggest that although 13-HODE incorporates into plasma and tissues, it is not likely to markedly alter endogenous pools due to its rapid turnover relative to the amount that gets incorporated. It is possible that changes in endogenous plasma or tissue OXLAM pools may be seen after prolonged periods of intake (>8 weeks) at relatively high dietary doses. To provide some context on exposure levels, average LNA intake in the US is ~16 g per person per day, whereas estimated OXLAM intake is in the order of milligrams [1,18]. Thus, despite the slower turnover of 13-HODE compared to fatty acids in peripheral tissues, dietary exposure to OXLAMs remains many orders of magnitude lower than fatty acids.

Hence, prolonged exposure to 13-HODE (or OXLAMs) may be necessary to alter tissue concentrations.

D4-13-HODE was not detected in either IV or gavaged brain samples, suggesting that the tracer did not accumulate in the brain. However, this does not exclude the possibility that d4-13-HODE entered the brain, but was rapidly metabolized by the time the tissue was dissected 90 min post tracer administration. Future studies should consider harvesting the brain shortly after continous infusion of the labeled 13-HODE tracer to steady-state levels in plasma [59], and following high-energy microwave fixation to avoid the effects of post-mortem ischemia [32].

In conclusion, this study demonstrated that ingested 13-HODE can be absorbed and incorporated into liver, heart, and adipose, and that these tissues preferentially derive 13-HODE from the ES plasma pool. Quantifying in vivo metabolism of 13-HODE and other oxylipin lipid mediators with tracers provides opportunities to understand metabolic and dietary factors regulating their concentration and bioactivity in vivo.

CRediT authorship contribution statement

Zhichao Zhang: Conceptualization, Formal analysis, Methodology, Investigation, Visualization, Writing - original draft. **Shiva Emami:** Methodology, Investigation. **Marie Hennebelle:** Conceptualization, Methodology, Investigation, Writing - review & editing. **Rhianna K. Morgan:** Investigation, Writing- original draft. **Larry A. Lerno:** Methodology, Resources, Writing - review & editing. **Carolyn M. Slupsky:** Conceptualization, Supervision, Resources, Writing - review & editing. **Pamela J. Lein:** Conceptualization, Supervision, Resources, Writing - review & editing. **Ameer Y. Taha:** Funding acquisition, Conceptualization, Methodology, Investigation, Supervision, Resources, Writing - review & editing.

Declaration of competing interest

The authors have no conflicts of interest to declare.

Acknowledgements

This work was supported by the USDA National Institute of Food and Agriculture, Hatch/Taha (project #1008787) and the Eunice Kennedy Shriver National Institute of Child Health and Human Development [grant number R21-HD095391-01A1). ZZ is a recipient of the Henry A. Jastro Research Award and MH is a recipient of the Graduate Women in Science Nell Mondy Fellowship.

Appendix A. Supplementary data

Supplementary data to this article can be found online at https://doi.org/10.1016/j.bbalip.2020.158870.

References

[1] T.L. Blasbalg, J.R. Hibbeln, C.E. Ramsden, S.F. Majchrzak, R.R. Rawlings, Changes in consumption of omega-3 and omega-6 fatty acids in the United States during the 20th century, Am. J. Clin. Nutr. 93 (2011) 950–962.

[2] W. Liu, H. Yin, Y.O. Akazawa, Y. Yoshida, E. Niki, N.A. Porter, Ex vivo oxidation in tissue and plasma assays of hydroxyoctadecadienoates: Z,E/E,E stereoisomer ratios, Chem. Res. Toxicol. 23 (2010) 986–995.

[3] O. Reinaud, M. Delaforge, J.L. Boucher, F. Rocchiccioli, D. Mansuy, Oxidative metabolism of linoleic acid by human leukocytes, Biochem. Biophys. Res. Commun. 161 (1989) 883–891.

[4] F. Engels, H. Willems, F.P. Nijkamp, Cyclooxygenase-catalyzed formation of 9-hydroxylinoleic acid by guinea pig alveolar macrophages under non-stimulated conditions, FEBS Lett. 209 (1986) 249–253.

[5] E.H. Oliw, Bis-allylic hydroxylation of linoleic-acid and arachidonic-acid by human hepatic monooxygenases, Biochim. Biophys. Acta 1166 (1993) 258–263.

[6] P.P. Halarnkar, R.N. Wixtrom, M.H. Silva, B.D. Hammock, Catabolism of epoxy fatty esters by the purified epoxide hydrolase from mouse and human liver, Arch. Biochem. Biophys. 272 (1989) 226–236.

[7] C.E. Ramsden, A.F. Domenichiello, Z.X. Yuan, M.R. Sapio, G.S. Keyes, S.K. Mishra, J.R. Gross, S. Majchrzak-Hong, D. Zamora, M.S. Horowitz, J.M. Davis, A. V. Sorokin, A. Dey, D.M. LaPaglia, J.J. Wheeler, M.R. Vasko, N.N. Mehta, A. J. Mannes, M.J. Iadarola, A systems approach for discovering linoleic acid derivatives that potentially mediate pain and itch, Sci. Signal. 10 (2017).

[8] A.Y. Taha, H.C. Blanchard, Y. Cheon, E. Ramadan, M. Chen, L. Chang, S. I. Rapoport, Dietary linoleic acid lowering reduces lipopolysaccharide-induced increase in brain arachidonic acid metabolism, Mol. Neurobiol. 54 (2017) 4303–4315.

[9] S. Schuster, C.D. Johnson, M. Hennebelle, T. Holtmann, A.Y. Taha, I.A. Kirpich, A. Eguchi, C.E. Ramsden, B.G. Papouchado, C.J. McClain, A.E. Feldstein, Oxidized linoleic acid metabolites induce liver mitochondrial dysfunction, apoptosis, and NLRP3 activation in mice, J. Lipid Res. 59 (2018) 1597–1609.

[10] M.F. Moghaddam, D.F. Grant, J.M. Cheek, J.F. Greene, K.C. Williamson, B. D. Hammock, Bioactivation of leukotoxins to their toxic diols by epoxide hydrolase, Nat. Med. 3 (1997) 562–566.

[11] S. Sugiyama, M. Hayakawa, S. Nagai, M. Ajioka, T. Ozawa, Leukotoxin, 9, 10-epoxy-12-octadecenoate, causes cardiac failure in dogs, Life Sci. 40 (1987) 225–231.

[12] M.D. Lynes, L.O. Leiria, M. Lundh, A. Bartelt, F. Shamsi, T.L. Huang, H. Takahashi, M.F. Hirshman, C. Schlein, A. Lee, L.A. Baer, F.J. May, F. Gao, N.R. Narain, E. Y. Chen, M.A. Kiebish, A.M. Cypess, M. Bluher, L.J. Goodyear, G.S. Hotamisligil, K. I. Stanford, Y.H. Tseng, Corrigendum: the cold-induced lipokine 12,13-diHOME promotes fatty acid transport into brown adipose tissue, Nat. Med. 23 (2017) 1384.

[13] M. Hennebelle, Z. Zhang, A.H. Metherel, A.P. Kitson, Y. Otoki, C.E. Richardson, J. Yang, K.S.S. Lee, B.D. Hammock, L. Zhang, R.P. Bazinet, A.Y. Taha, Linoleic acid participates in the response to ischemic brain injury through oxidized metabolites that regulate neurotransmission, Sci. Rep. 7 (2017) 4342.

[14] M. Hennebelle, R.K. Morgan, S. Sethi, Z. Zhang, H. Chen, A.C. Grodzki, P.J. Lein, A. Y. Taha, Linoleic acid-derived metabolites constitute the majority of oxylipins in the rat pup brain and stimulate axonal growth in primary rat cortical neuron-glia co-cultures in a sex-dependent manner, J. Neurochem. 152 (2) (2019) 195–207.

[15] C.E. Ramsden, A. Ringel, A.E. Feldstein, A.Y. Taha, B.A. MacIntosh, J.R. Hibbeln, S. F. Majchrzak-Hong, K.R. Faurot, S.I. Rapoport, Y. Cheon, Y.M. Chung, M. Berk, J. D. Mann, Lowering dietary linoleic acid reduces bioactive oxidized linoleic acid metabolites in humans, Prostaglandins Leukot Essent Fatty Acids 87 (2012) 135–141.

[16] C.E. Ramsden, M. Hennebelle, S. Schuster, G.S. Keyes, C.D. Johnson, I.A. Kirpich, J. E. Dahlen, M.S. Horowitz, D. Zamora, A.E. Feldstein, C.J. McClain, B. S. Muhlhausler, M. Makrides, R.A. Gibson, A.Y. Taha, Effects of diets enriched in linoleic acid and its peroxidation products on brain fatty acids, oxylipins, and aldehydes in mice, Biochim. Biophys. Acta Mol. Cell Biol. Lipids 1863 (2018) 1206–1213.

[17] A.Y. Taha, M. Hennebelle, J. Yang, D. Zamora, S.I. Rapoport, B.D. Hammock, C. E. Ramsden, Regulation of rat plasma and cerebral cortex oxylipin concentrations with increasing levels of dietary linoleic acid, Prostaglandins Leukot Essent Fatty Acids 138 (2018) 71–80.

[18] C.E. Richardson, M. Hennebelle, Y. Otoki, D. Zamora, J. Yang, B.D. Hammock, A. Y. Taha, Lipidomic analysis of oxidized fatty acids in plant and algae oils, J. Agric. Food Chem. 65 (2017) 1941–1951.

[19] J.A. Gan, Z. Zhang, K. Kurudimov, J.B. German, A.Y. Taha, Distribution of free and esterified oxylipins in cream, cell, and skim fractions of human milk, Lipids 55 (6) (2020) 661–670.

[20] F.F.G. Dias, T.R. Augusto-Obara, M. Hennebelle, S. Chantieng, G. Ozturk, A. Y. Taha, T. Vieira, J.M. Leite Nobrega de Moura Bell, Effects of industrial heat treatments on bovine milk oxylipins and conventional markers of lipid oxidation, Prostaglandins Leukot. Essent. Fatty Acids 152 (2020) 102040.

[21] M.A. Pitino, S.M. Alashmali, K.E. Hopperton, S. Unger, Y. Pouliot, A. Doyen, D. L. O'Connor, R.P. Bazinet, Oxylipin concentration, but not fatty acid composition, is altered in human donor milk pasteurised using both thermal and non-thermal techniques, Br. J. Nutr. 122 (2019) 47–55.

[22] N. Kalogeropoulos, F.N. Salta, A. Chiou, N.K. Andrikopoulos, Formation and distribution of oxidized fatty acids during deep- and pan-frying of potatoes, Eur J Lipid Sci Tech 109 (2007) 1111–1123.

[23] J.G. Bergan, H.H. Draper, Absorption and metabolism of 1-14C-methyl linoleate hydroperoxide, Lipids 5 (1970) 976–982.

[24] K. Kanazawa, H. Ashida, Dietary hydroperoxides of linoleic acid decompose to aldehydes in stomach before being absorbed into the body, Biochim. Biophys. Acta 1393 (1998) 349–361.

[25] J. Glavind, C. Sylven, Intestinal absorption and lymphatic transport of methyl linoleate hydroperoxide and hydroxyoctadecadienoate in the rat, Acta Chem. Scand. 24 (1970) 3723–3728.

[26] C.E. Ramsden, A. Ringel, S.F. Majchrzak-Hong, J. Yang, H. Blanchard, D. Zamora, J.D. Loewke, S.I. Rapoport, J.R. Hibbeln, J.M. Davis, B.D. Hammock, A.Y. Taha, Dietary Linoleic Acid-induced Alterations in pro- and Anti-nociceptive Lipid Autacoids: Implications for Idiopathic Pain Syndromes? *Mol Pain* 12, 2016.

[27] Lundstrom, S. L., B. Levanen, M. Nording, A. Klepczynska-Nystrom, M. Skold, J. Z. Haeggstrom, J. Grunewald, M. Svartengren, B. D. Hammock, B. M. Larsson, A. Eklund, A. M. Wheelock, and C. E. Wheelock. 2011. Asthmatics Exhibit Altered Oxylipin Profiles Compared to Healthy Individuals after Subway Air Exposure. *Plos One* 6.

[28] N.C. Long, A. Morimoto, T. Nakamori, O. Yamashiro, N. Murakami, Intraperitoneal injections of prostaglandin E2 attenuate hyperthermia induced by restraint or interleukin-1 in rats, J. Physiol. 444 (1991) 363–373.

[29] O. Quehenberger, S. Dahlberg-Wright, J. Jiang, A.M. Armando, E.A. Dennis, Quantitative determination of esterified eicosanoids and related oxygenated metabolites after base hydrolysis, J. Lipid Res. 59 (2018) 2436–2445.

[30] A.I. Ostermann, E. Koch, K.M. Rund, L. Kutzner, M. Mainka, N.H. Schebb, Targeting esterified oxylipins by LC-MS - effect of sample preparation on oxylipin pattern, Prostaglandins Other Lipid Mediat 146 (2020) 106384.
[31] M. Schwab, R. Bauer, U. Zwiener, The distribution of normal brain water content in Wistar rats and its increase due to ischemia, Brain Res. 749 (1997) 82–87.
[32] M. Hennebelle, A.H. Metherel, A.P. Kitson, Y. Otoki, J. Yang, K.S.S. Lee, B. D. Hammock, R.P. Bazinet, A.Y. Taha, Brain oxylipin concentrations following hypercapnia/ischemia: effects of brain dissection and dissection time, J. Lipid Res. 60 (2019) 671–682.
[33] Z.X. Yuan, S.I. Rapoport, S.J. Soldin, A.T. Remaley, A.Y. Taha, M. Kellom, J. Gu, M. Sampson, C.E. Ramsden, Identification and profiling of targeted oxidized linoleic acid metabolites in rat plasma by quadrupole time-of-flight mass spectrometry, Biomed. Chromatogr. 27 (2013) 422–432.
[34] C.T. Chen, A.P. Kitson, K.E. Hopperton, A.F. Domenichiello, M.O. Trepanier, L. E. Lin, L. Ermini, M. Post, F. Thies, R.P. Bazinet, Plasma non-esterified docosahexaenoic acid is the major pool supplying the brain, Sci. Rep. 5 (2015) 15791.
[35] B. Samuelsson, Prostaglandins and related factors. 27. Synthesis of tritium-labeled prostaglandin E1 and studies on its distribution and excretion in the rat, J. Biol. Chem. 239 (1964) 4091–4096.
[36] A. Raz, Metabolities formed after intravenous administration of free or albumin-bound prostaglandin E 2 in the rat, FEBS Lett. 27 (1972) 245–247.
[37] H.B. Lee, M.D. Blaufox, Blood volume in the rat, J. Nucl. Med. 26 (1985) 72–76.
[38] Y.H. Cho, V.A. Ziboh, Incorporation of 13-Hydroxyoctadecadienoic acid (13-Hode) into epidermal ceramides and phospholipids - phospholipase C-catalyzed release of novel 13-Hode-containing diacylglycerol, J. Lipid Res. 35 (1994) 255–262.
[39] L.M. Rodriguez-Alcala, I. Ares, J. Fontecha, M.R. Martinez-Larranaga, A. Anadon, M.A. Martinez, Absorption kinetics of the main conjugated linoleic acid isomers in commercial-rich oil after oral administration in rats, J Agr Food Chem 65 (2017) 7680–7686.
[40] Borgstrom, B., and T. Olivecrona. 1961. Metabolism of Palmitic Acid-L-C14 in Functionally Hepatectomized Rats. *Journal of Lipid Research* 2: 263-&.
[41] K. Strassburg, D. Esser, R.J. Vreeken, T. Hankemeier, M. Muller, J. van Duynhoven, J. van Golde, S.J. van Dijk, L.A. Afman, D.M. Jacobs, Postprandial fatty acid specific changes in circulating oxylipins in lean and obese men after high-fat challenge tests, Mol. Nutr. Food Res. 58 (2014) 591–600.
[42] A.I. Ostermann, T. Greupner, L. Kutzner, N.M. Hartung, A. Hahn, J.P. Schuchardt, N.H. Schebb, Intra-individual variance of the human plasma oxylipin pattern: low inter-day variability in fasting blood samples versus high variability during the day, Anal Methods-Uk 10 (2018) 4935–4944.
[43] Rapoport, S. I., and A. Taha. 2014. Imaging Brain DHA Metabolism in Vivo, in Animals, and Humans. *Omega-3 Fatty Acids in Brain and Neurological Health*: 265-275.
[44] P.J. Robinson, S.I. Rapoport, A method for examining turnover and synthesis of palmitate-containing brain lipids in vivo, Clin. Exp. Pharmacol. Physiol. 16 (1989) 701–714.
[45] H.R. Modi, A.Y. Taha, H.W. Kim, L. Chang, S.I. Rapoport, Y. Cheon, Chronic clozapine reduces rat brain arachidonic acid metabolism by reducing plasma arachidonic acid availability, J. Neurochem. 124 (2013) 376–387.
[46] S.I. Rapoport, M.C. Chang, A.A. Spector, Delivery and turnover of plasma-derived essential PUFAs in mammalian brain, J. Lipid Res. 42 (2001) 678–685.
[47] X. Fang, T.L. Kaduce, A.A. Spector, 13-(S)-hydroxyoctadecadienoic acid (13-HODE) incorporation and conversion to novel products by endothelial cells, J. Lipid Res. 40 (1999) 699–707.
[48] L. Balas, P. Rise, D. Gandrath, G. Rovati, C. Bolego, F. Stellari, A. Trenti, C. Buccellati, T. Durand, A. Sala, Rapid Metabolization of Protectin D1 by beta-oxidation of its polar head chain, J. Med. Chem. 62 (2019) 9961–9975.
[49] L.G.J. Cayer, A.M. Mendonca, S.D. Pauls, T. Winter, S. Leng, C.G. Taylor, P. Zahradka, H.M. Aukema, Adipose tissue oxylipin profiles vary by anatomical site and are altered by dietary linoleic acid in rats, Prostaglandins Leukot Essent Fatty Acids 141 (2019) 24–32.
[50] H. Suganuma, A.J. McPhee, C.T. Collins, G. Liu, S. Leemaqz, C.C. Andersen, N. Ikeda, N. Ohkawa, A.Y. Taha, R.A. Gibson, Intravenous fat induces changes in PUFA and their bioactive metabolites: comparison between Japanese and Australian preterm infants, Prostaglandins Leukot Essent Fatty Acids 102026 (2019).
[51] M.O. Trepanier, K.M. Kwong, A.F. Domenichiello, C.T. Chen, R.P. Bazinet, W. M. Burnham, Intravenous infusion of docosahexaenoic acid increases serum concentrations in a dose-dependent manner and increases seizure latency in the maximal PTZ model, Epilepsy Behav. 50 (2015) 71–76.
[52] B.L. Hungund, Z. Zheng, A.I. Barkai, Turnover of ethyl-linoleate in rat plasma and its distribution in various organs, Alcohol. Clin. Exp. Res. 19 (1995) 374–377.
[53] M. Hamberg, B. Samuelsson, On the metabolism of prostaglandins E 1 and E 2 in man, J. Biol. Chem. 246 (1971) 6713–6721.
[54] H.K. Shrestha, M.A. Beg, R.R. Burnette, O.J. Ginther, Plasma clearance and half-life of prostaglandin F2alpha: a comparison between mares and heifers, Biol. Reprod. 87 (2012).
[55] E.J. Murphy, G. Barcelo-Coblijn, B. Binas, J.F. Glatz, Heart fatty acid uptake is decreased in heart fatty acid-binding protein gene-ablated mice, J. Biol. Chem. 279 (2004) 34481–34488.
[56] M. Igarashi, L. Chang, K. Ma, S.I. Rapoport, Kinetics of eicosapentaenoic acid in brain, heart and liver of conscious rats fed a high n-3 PUFA containing diet, Prostaglandins Leukot Essent Fatty Acids 89 (2013) 403–412.
[57] A.H. Metherel, R.J.S. Lacombe, R. Chouinard-Watkins, K.E. Hopperton, R. P. Bazinet, Complete assessment of whole-body n-3 and n-6 PUFA synthesis-secretion kinetics and DHA turnover in a rodent model, J. Lipid Res. 59 (2018) 357–367.
[58] A.F. Domenichiello, A.P. Kitson, C.T. Chen, M.O. Trepanier, P.M. Stavro, R. P. Bazinet, The effect of linoleic acid on the whole body synthesis rates of polyunsaturated fatty acids from alpha-linolenic acid and linoleic acid in free-living rats, J. Nutr. Biochem. 30 (2016) 167–176.
[59] A.Y. Taha, L. Chang, M. Chen, Threshold changes in rat brain docosahexaenoic acid incorporation and concentration following graded reductions in dietary alpha-linolenic acid, Prostaglandins Leukot Essent Fatty Acids 105 (2016) 26–34.